Modern Physics Letters B
(2024) 2450056 (15 pages)
© World Scientific Publishing Company
DOI: 10.1142/S0217984924500568

Mod. Phys. Lett. B Downloaded from www.worldscientific.com
by BILKENT UNIVERSITY on 01/03/24. Re-use and distribution is strictly not permitted, except for Open Access articles.

Investigation of resonant properties of metamaterial THz filters fabricated from vanadium dioxide thin films

Sehriban Zeybek*, Yasemin Demirhan† and Aileen Noori‡

Department of Physics, Izmir Institute of Technology,
Urla, Izmir 35430, Turkey
**sehribanzeybek@gmail.com*
†*yasemindemirhan@iyte.edu.tr*
‡*aileennoori@iyte.edu.tr*

Halime Tugay§ and Hakan Altan¶

Department of Physics, Middle East Technical University,
Çankaya, Ankara 06800, Turkey
§*halimetugay@gmail.com*
¶*haltan@metu.edu.tr*

Cumali Sabah

Electrical and Electronics Engineering,
Middle East Technical University-Northern Cyprus Campus (METU-NCC),
Kalkanli, Guzelyurt 99738, Mersin 10, Turkey
sabah@metu.edu.tr

Gulnur Aygun‖ and Lutfi Ozyuzer**

Department of Physics, Izmir Institute of Technology,
Urla, Izmir 35430, Turkey
‖*gulnuraygun@iyte.edu.tr*
***lutfiozyuzer@iyte.edu.tr*

Received 15 May 2023
Revised 29 July 2023
Accepted 4 August 2023
Published 21 October 2023

Vanadium dioxide (VO_2) is a promising candidate for electronic and optical switching applications in the terahertz frequency range due to the metal to insulator transition (MIT). In this study, the use of VO_2 patterned as a metamaterial surface or coupled as a homogeneous layer with a metallic metamaterial surface on top is investigated in terms of performance. High-quality VO_2 thin films were deposited on c-cut sapphire substrates by using the dc magnetron sputtering technique. A change in resistivity by a factor of 10^4 MIT in VO_2 was observed allowing to investigate its use as a controllable metamaterial. The layer was patterned using a unique geometry (four-cross shaped) that operates in the THz frequency range. To understand its performance as a tunable THz filter, the four-cross structure fabricated from VO_2

† Corresponding author.

is compared to one fabricated from Au on VO_2 bare film using UV lithography and ion beam etching techniques. The spectral performances of metamaterials were assessed using THz-Time Domain Spectroscopy (THz-TDS) and results were compared with simulations based on CST Microwave Studio. Absence of the resonant effects in the purely developed VO_2 device, while clear observation of the MIT behavior shows the strong dependency of the inductive and/or capacitive effects of the four-cross structure on conductivity of the surface metamaterial, which is clearly observable for the Au-based device. In the latter case, the resonant transmittance of the filter can be effectively modulated by change in temperature.

Keywords: THz metamaterials; VO_2 thin film; tunable metamaterials; metal-insulating transition (MIT) materials.

Mod. Phys. Lett. B Downloaded from www.worldscientific.com
by BILKENT UNIVERSITY on 01/03/24. Re-use and distribution is strictly not permitted, except for Open Access articles.

1. Introduction

Terahertz (THz) radiation lies in the region of the electromagnetic spectrum which is between microwaves and the infrared. Since it is difficult to develop devices which can interact, generate or detect radiation due to the typically weak electromagnetic response of bulk materials in the frequency range between 0.1 and 10 THz, this region is usually called the THz gap. There are important efforts focusing to fill this vacancy in the spectrum.[1–11] Due to their latent utilizations in security monitoring (THz imaging), non-destructive testing, wireless communications, and material characterization metamaterials manipulating light in the THz regime have drawn great attention. Metamaterials whose resonant interactions can be realized through ring-like periodic surface structures in this frequency range initially allowed the development of passive THz filter devices based on conductive metals patterned on dielectric media. Materials whose conductivity can be controlled employed with such metal patterned structures have shown promise as tunable THz filters, but patterning of such materials into metamaterial devices by themselves has been challenging. One exception has been superconducting metamaterials, although their practical employment is elaborate due to the cooling requirements and the power necessary to maintain these systems. The demand to fabricate devices that operate in this frequency range closer to the room temperature has driven recent investigations. One of the basic outcomes of strongly correlated material research is phase transition phenomena. Due to extensive technological capabilities awarded through controllable optical, electronic, and structural properties, there have been various attempts to implement the transition properties of novel materials in various architectures.[11–16] Transition metal oxides, such as vanadium oxides, show the insulator-to-metal transition (MIT) behavior near room temperature, so that it can be a versatile material for temperature sensitive photonic and electronic devices. Curiously enough, there are variations between oxides of vanadium and among them VO_2 has the nearest transition to room temperature. Due to its substantial change in optical and electrical properties as a result of structural phase change from a semiconducting monoclinic phase (low-temperature) to a metallic tetragonal phase (high-temperature) at $\sim 68^{\circ}$C VO_2 has been recognized as an excellent tunable functional material.[16–21] The transition speed for the electrical activation is in the order of

Mod. Phys. Lett. B Downloaded from www.worldscientific.com
by BILKENT UNIVERSITY on 01/03/24. Re-use and distribution is strictly not permitted, except for Open Access articles.

nanoseconds whereas the optical-induced transition reduces to the picosecond and femtosecond regimes. Substantial attempts have taken place in fabricating frequency tunable metamaterials displaying narrow-band operation for a certain part of the electromagnetic spectrum, including microwave,[21] THz[22] and optical frequencies[23–25] using the phase changing properties of VO_2. For metamaterial devices based on split ring resonators, modulation of the resonant THz beam transmission was controlled through the conductive behavior of the SRR gap which transitioned from capacitive to resistive with the help of thermal triggering of the phase change of VO_2.[25–30]

A great number of these studies have concentrated on tunable THz metamaterials based on the phase transition of VO_2 triggered by temperature tuning, however, since VO_2 is a superior quality photoelectric functional material it displays a distinctive transition property that can be onset not just by heat but by the external excitation of light, or stress.[31]

In this study, two types of metamaterial filters are produced. One is fabricated by patterning planar VO_2 films (referred as "four-cross-planar VO_2 device") and the other is constructed from patterning Au on VO_2 films (referred as "Au four-cross patterned VO_2 device"). By tuning between insulating and metallic phases of the VO_2 layer, the frequency-dependent THz transmission spectra of both metamaterial designs are demonstrated and compared. The four-cross planar VO_2 device exhibited a non-resonant change in transmission absent of any expected resonant features while the Au four-cross patterned VO_2 device showed an observable change near the expected resonant transmission with change in temperature. The strong dependency of the quality factor of the resonance on the dielectric properties of the medium is evident in these investigations, and that conductivity or sheet resistance of the VO_2 film is not enough to simulate the observed transmission in the THz range. There are still many approaches and ongoing studies to construct the suitable and efficient metamaterials combined with phase change VO_2 material. The performance comparison of two types of metamaterial devices that given in study will give an insight to the development of such devices.

2. Experimental Results

2.1. *Background & modeling*

In order to quantify the temperature dependent transmission characteristics and also validate the filter properties of the designed metamaterial structure, simulations were performed using the commercial software CST Microwave Studio suite (version 2019) program. Unit cell boundary condition is used with the Frequency Domain Simulator and the linearly polarized plane wave is propagated at normal incidence to the surface. Previous investigations by our group have shown that the "four-cross" structure can be utilized as a terahertz filter operating in the sub-THz frequency range.[32] A detailed demonstration of the filter structure is presented in Figs. 1(a) and 1(b) for the four-cross-planar VO_2 device and Au four-cross patterned VO_2 device, respectively.

Mod. Phys. Lett. B Downloaded from www.worldscientific.com
by BILKENT UNIVERSITY on 01/03/24. Re-use and distribution is strictly not permitted, except for Open Access articles.

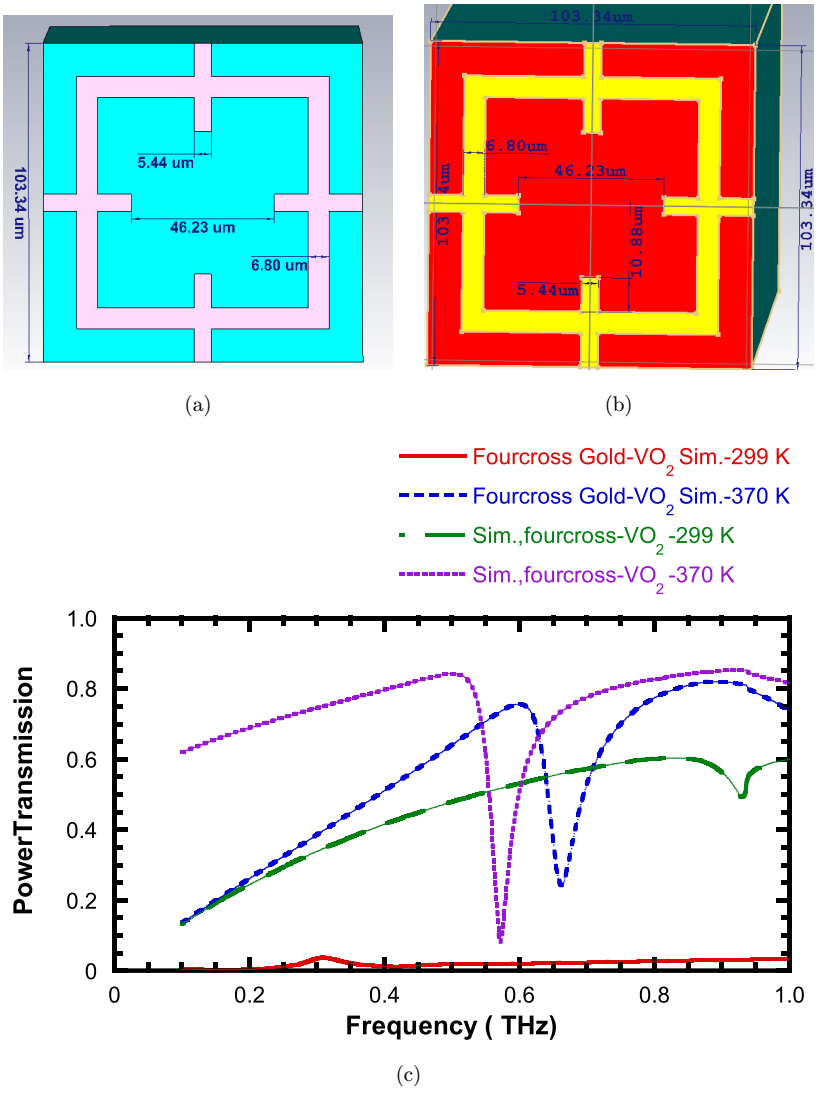


Fig. 1. (Color online) (a) Detailed demonstration of the four-cross-planar VO_2 device with designed parameters. (b) Detailed demonstration of the Au four-cross patterned VO_2 device with designed parameters. (c) The simulated transmission spectrum of the four-cross-planar VO_2 device and the four-cross-planar VO_2 device at 299 and 370 K respectively.

The structure of the metamaterial, which was comprised by a four-cross rectangular resonator, has a rectangular shape in which band lines are placed at the sides of the ring on a dielectric substrate. The unique pattern, a conjunction of a square ring with four-fold strips, allows for the necessary capacitive an inductive interaction typically seen with split-ring resonator structures. Simulations were performed using frequency domain approach in CST Microwave Studio for the region 0.01–1 THz.

Mod. Phys. Lett. B Downloaded from www.worldscientific.com
by BILKENT UNIVERSITY on 01/03/24. Re-use and distribution is strictly not permitted, except for Open Access articles.

Both devices utilize a 250 nm thick VO_2 layer grown on a 500 μm thick sapphire substrate. Supported by THz-TDS measurements, an electrical permittivity value of $\varepsilon_r = 9.61$ was assumed to be constant in this frequency region for the sapphire substrate. Likewise, the VO_2 layer is assumed to be lossless and have a dielectric permittivity of $\varepsilon_r = 9$ at room temperature. Its temperature-dependent dielectric parameters, which are supported by THz-TDS measurements on an unpatterned VO_2 layer grown on dielectric saphhire substrate is modeled following the Bruggeman effective medium approach based on a Boltzmann function to model the volume fraction (V) of the metallic domains.[33]

$$VO_2 = \frac{1}{4}\{\varepsilon_d(2-3V) + \varepsilon_m(3V-1)\sqrt{[\varepsilon_d(2-3V) + \varepsilon_m(3V-1)]2 + 8\varepsilon_d\varepsilon_m}\}. \quad (1)$$

In this model, the dielectric function for the VO_2 layer in the metallic state (ε_m) is based on a Drude model.[34] In Fig. 1(c), the numerical results for terahertz wave transmittance of both devices are presented. The primary simulated results for the etched four-cross structure on a VO_2 layer and the one where gold is patterned in the exact same four-cross pattern on a VO_2 layer yield terahertz wave minimum transmittance peaks at around 0.56 THz and 0.65 THz, respectively.

2.2. *VO_2 film growth*

There are various methods utilized in the preparation of VO_2 thin films such as sol–gel,[34] pulse laser deposition,[35] thermal evaporation,[36] sputtering[37,38] and others. One of the preparation methods extensively employed is magnetron sputtering which is introduced due to superiority of films in high packing density, uniformity, good adhesion, and effortlessly for industrialization. Many current efforts are concentrated on understanding the mechanism of the phase transition and subsequent modification of the transition performance of VO_2 films.[25,36] Onset of MIT in the films is extremely dependent to deposition parameters, namely, sputtering power, deposition rate, oxygen partial pressure, and substrate temperature. In our previous studies, to obtain VO_2 single phase, ideal growth parameters were investigated by the help of XRD, RAMAN and XPS analysis.[37,38] There are many variables such as substrate, growth temperature, deposition rate and sputtered ion energy affecting the quality of the grown vanadium oxide films. In this study, the optimum growth conditions are used for VO_2 film deposition. VO_2 exhibits metal insulator transition (MIT) at around 70°C. VO_2 shows insulator phase at low temperature whereas above the transition temperature VO_2 shows metallic phase. The resistivity of this material abruptly changes by a factor of 10^4 at the MIT temperature. It is known that mixed phases of vanadium oxide systems need to be optimized in terms of sputtering parameters to yield high quality pure VO_2 phase. One of the most crucial property that indicates the film quality is the resistivity drop at T_{MIT}.

Unlike other phase change materials, the conductivity of VO_2 can be increased by 4, 5 orders of magnitude under external stimulus such as applied electric fields as well as optical and thermal pumping.[38]

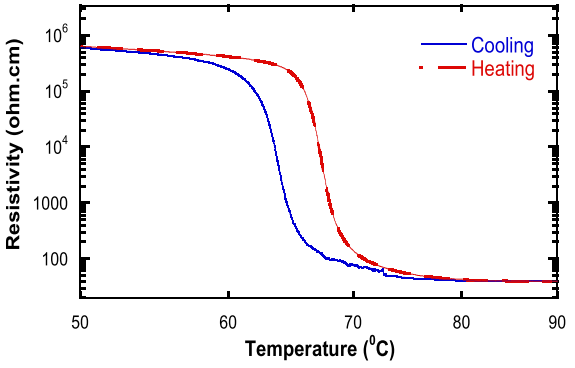


Fig. 2. (Color online) The MIT hysteresis behavior of the unpatterned VO_2 samples at $\sim 68°C$.

In the development process, thin film deposition, photolithography and ion beam etching techniques were used for the microfabrication of the metamaterial filters. DC magnetron sputtering technique was employed where high purity (99.95%) vanadium (V) target was used for the deposition of VO_2 thin films on c-cut sapphire (Al_2O_3 (0001)).[38] With the help of ultrasonic cleaner, cleaning of the substrates was carried out using acetone and DI water. In the deposition process, evacuation of the vacuum chamber up to a base pressure of 1.2×10^{-6} mbar was realized, meanwhile a temperature of 550°C was attained for the sapphire substrates. A former process to deposition was introduced on the target by pre-sputtering for 10 min with the purpose of removing any contaminations of target's surface. The fabrication of VO_2 thin films was carried out under the circumstances where 8.5×10^{-3} mbar of O_2 and Ar mixed gas pressure and 50 W of sputtering power were accomplished. In the course of deposition, for the purpose of uniformity development in the film, a rotation of the substrates with 15 rpm was provided. Oxygen gas ratio of the sputtered thin films was altered in accordance with the exploration of the growth circumstances of VO_2 thin films maintaining sharp resistivity changes at MIT. Electrical properties of the VO_2 samples were characterized using a microprobe station under vacuum environment. MIT with hysteresis behavior was observed for the unpatterned samples at $\sim 68°C$ (Fig. 2).

VO_2 exhibits a reversible MIT at around 68°C. It has been shown that MIT behavior of VO_2 strongly depends on wide range with crystal quality, grain size, grain boundaries and defects related to self-doping and the other factors.[38,39] While VO_2 has monoclinic crystal structure with insulator phase at below the MIT temperature (TMIT), the material has tetragonal rutile crystal structure with metallic phase at above TMIT. During the MIT transition, the change in the volume of VO_2 crystal is approximately 1%–2%. In insulator phase, the energy bandgap of VO_2 is around 0.65 Ev. There have been two theories to explain the hysterisis loop characteristics of MIT in VO_2; Peierles transition and Mott–Hubbard transition. Peierles transition arises due to the change in crystal structure, and Mott–Hubbard transition takes places due to electron–electron correlations.

Mod. Phys. Lett. B Downloaded from www.worldscientific.com
by BILKENT UNIVERSITY on 01/03/24. Re-use and distribution is strictly not permitted, except for Open Access articles.

Mod. Phys. Lett. B Downloaded from www.worldscientific.com
by BILKENT UNIVERSITY on 01/03/24. Re-use and distribution is strictly not permitted, except for Open Access articles.

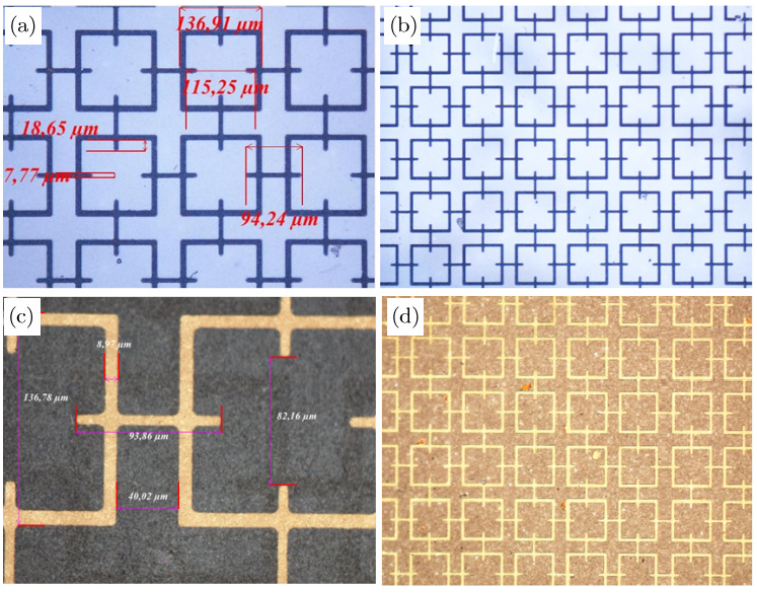


Fig. 3. (Color online) (a), (c) Optical microscope images of four-cross-planar VO_2 device and Au four-cross patterned VO_2 device given with measured dimensions. (b), (d) Optical microscope images of four-cross-planar VO_2 device and Au four-cross patterned VO_2 device which is taken with different magnifications.

After the thin film deposition, THz four-cross metamaterial filters were fabricated using the UV photolithography and Ar ion beam etching techniques. During the UV lithography process, different imperfections could appear as irregularity in shape rounding, etc. Figures 3(a)–(d) show the optical photographs of the fabricated metamaterial filters patterned by etching the VO_2 layer and patterned by depositing gold on bare VO_2 layer, respectively.

2.3. *THz time domain measurements*

A home-built terahertz time-domain spectroscopy (THz-TDS) system was employed in order to analyze the transmission characteristics of the realized THz four-cross metamaterial filters. Two optical beam lines of the spectrometer are used in an interferometric configuration, in which one is called the generation arm and the other the detection arm. A photo-conductive antenna is used to generate a *s*-polarized terahertz beam. By making use of two off-axis parabolic mirrors and two TPX lenses, the beam is guided and collected to and from the sample. A focal spot diameter of roughly 5 mm on the sample is achieved. Measurement of the THz pulse is done using electro-optical detection based on a ZnTe crystal and a balanced photodetector.

Using phase sensitive lock-in detection, the data is collected with and without the samples with the help of a personal computer. Subsequent Fourier analysis resulted in a frequency resolution of 40 GHz. Temperature-dependent measurements were carried out using a home-built heater that is calibrated for measurements up to 370 K.

Mod. Phys. Lett. B Downloaded from www.worldscientific.com
by BILKENT UNIVERSITY on 01/03/24. Re-use and distribution is strictly not permitted, except for Open Access articles.

3. Results and Discussion

Requirement of the optimization of mixed phases for vanadium oxide systems in concern with sputtering parameters in order to produce high quality pure VO_2 phase has been recognized. The resistivity drop at MIT is among the virtually significant characteristics in determination of film quality. It is pointed out that uniformity of the film, strain, grain size and boundaries are the dependant of the change in resistivity. In the measurement region 30°C and 90°C, the resistivity of the bare VO_2 films is presented in Fig. 2. At transition temperature, an evident decrease in the resistivity of bare film with greater than $\sim 10^4$ of magnitude has been observed. In the case of this bare thin film sample, MIT value is around 68°C, and the hysteresis loop width is around 4°C and for DC sputtered high quality VO_2 thin films they are entirely acceptable values. Furthermore, the abrupt MIT in VO_2 allows the amplitude variation of the resonant peaks of a metamaterial switching device on an extremely short temperature region. In the VO_2 transitional state, the film constitutes nanoscale configurations of metallic- and insulator-state VO_2, and the developing medium operates as a tunable irregular metamaterial. A beneficial usage of this attitude could be a thermally triggered electrical switch which may operate by supplying minute; however, momentary heat pulses additionally cooling pulses of small amplitudes with the rank of a few Kelvins.

The measured transmission spectra of four-cross VO_2 metamaterial filter (Four-cross (VO_2)) at 299, 310, 330, 340, 350, 370 K are given in Fig. 4. The observed oscillations are by virtue of the etalon effect and turn to be more evident with increasing temperature.

The ratio between the Fourier-transformed amplitude spectra of the sample and the heated stage with no sample mounted specified the frequency-dependent transmission. Accordingly, the measured transmission spectra incorporated the Fabry–Perot resonance effect taking place from the Al_2O_3 substrate (0.5 mm thick). In the case when the critical temperature of the VO_2 sample is over 340 K the aforementioned

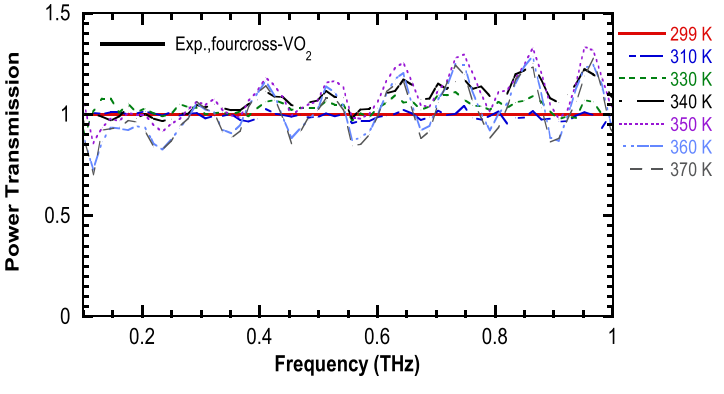


Fig. 4. (Color online) THz time-domain measurements of four-cross-planar VO_2 device at 299, 310, 330, 340, 350, 360 and 370 K.

Mod. Phys. Lett. B Downloaded from www.worldscientific.com
by BILKENT UNIVERSITY on 01/03/24. Re-use and distribution is strictly not permitted, except for Open Access articles.

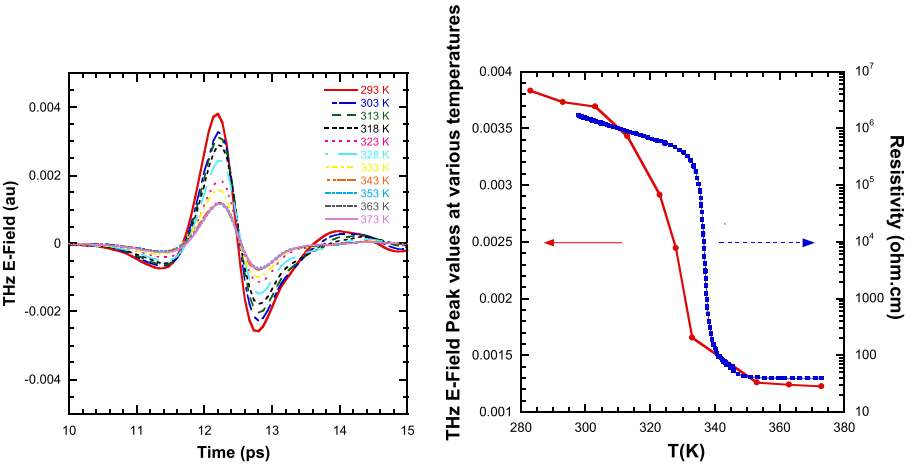
effect becomes apparent to a greater extent. Furthermore, one could declare that the sample is an insulator providing that the temperature is under the critical temperature and on the other hand in the case when the temperature is over the critical temperature the sample is metallic where the THz radiation adding to the observed dips in the etalon is demonstrated. Even though the metamaterial configuration incorporating rectangular loops does not demonstrate any resonant properties the broadband THz transmission can be entirely turned off/on. At room temperature the dielectric constant of VO_2 is approximately 9 (insulating state) and when MIT occurs, the structural transformation occurs and VO_2 turns into the rutile phase. The formation of the undesirable structural inhomogeneity provokes a monoclinic metal phase as an intermediate state that appears in a region between the MIT and the structural phase transition temperatures (SPT). This phenomenon can cause a highly anisotropic THz dielectric function of VO_2 films which can affect the resonance of the metamaterial device strongly. Metamaterial device research recently has focused on development of advanced structures based on functional materials. Due to complexity of the overall metamaterial structure, e.g. chiral metamaterials, resultant device architecture may not manipulate the incident radiation effectively using optical and/or electrical means. Noting that the lower conductivity of VO_2 compared to a pure metal is not sufficient to manipulate the incident radiation for patterned VO_2 designs, a second design was implemented in order to better observe resonant THz interactions. Among the research areas of metamaterials, there exists a driving aspect namely; together with the optical resonance, the extensive utilization of nano-engineered metals has been documented to entitled complex functionalities that furnishes the basis for accomplishing "self-sufficient" metadevices. Nevertheless, an immediate investigation of the documented chiral metamaterials exposes that most patterns cannot endorse the extra functionalities due to the fact that they conventionally comprise of geometrically isolated units.

This second device comprising of one identical four-cross design with a structure equivalent to the one illustrated beforehand is produced that is supported by the metallic structure. Characterized by time-domain THz measurement systems this design showed more pronounce resonant effects. In Fig. 5(a), it can be noticed that when bare VO_2 thin film changes between the insulating and the metallic state, amplitude of the electric field of the transmitted wave varies significantly. Also, in Fig. 5(b), the THz electric field peak to peak value is plotted with respect to temperature, showing this transition clearly.

Including semiconducting and metallic phases of VO_2 film the frequency-dependent transmission spectra of our second design, Au/VO_2 four-cross structure layer at 293, 303, 313, 318, 323, 328, 333, 343, 353, 363, and 373 K is shown in Fig. 6.

It is obviously seen from the terahertz measurement of the frequency selective surface composed of shaped gold layer that the resonance (0.7 THz) disappears around the VO_2 transition temperature. In Fig. 6, it is seen that with a decrease in temperature, one observes increase in resonance strength and also a resonance shift to higher frequencies. With the increase of temperature (from 273 K up to MIT)

Mod. Phys. Lett. B Downloaded from www.worldscientific.com
by BILKENT UNIVERSITY on 01/03/24. Re-use and distribution is strictly not permitted, except for Open Access articles.



(a) (b)

Fig. 5. (Color online) (a) The amplitude of the electric field of the transmitted wave versus time graph. (b) The THz E-field peak values versus temperature curve is plotted in order to determine the MIT temperature of the VO_2 film (red curve). The MIT measurement of the film is also plotted on the same graph (blue curve).

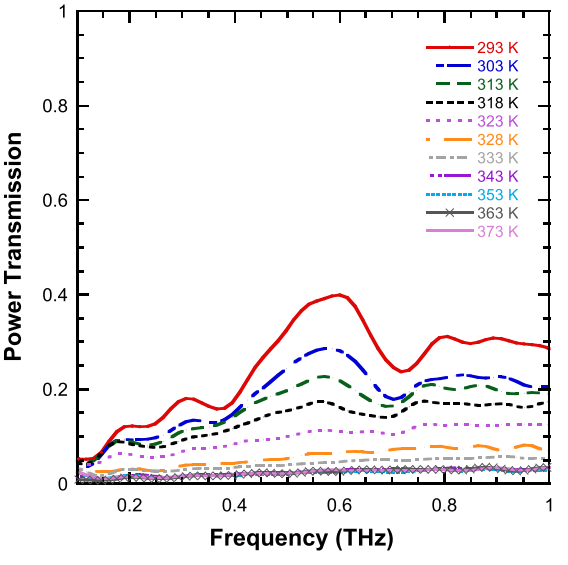


Fig. 6. (Color online) THz time-domain measurement of four-cross-planar VO_2 device taken from 293 to 373 K.

resonance frequency is blue-shifted and it is observed that the resonance strength disappeared as a broadening and reduction in amplitude of the transmission dip. In the present circumstance, as presented in Fig. 5, it is observed that low-lying second resonance frequency (around 0.370 THz) takes place close to the resonance frequency

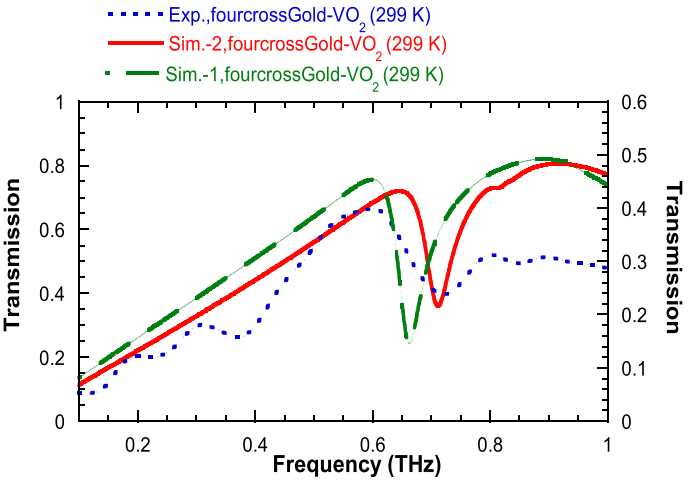


Fig. 7. (Color online) THz time-domain measurement of four-cross-planar VO_2 device at 299 K, plotted with simulation results (The initial simulation results and the repeated simulation results in compliance with measured unitcell parameters (Sims. 1 and 2.)) on the same graph.

of the four-cross gold/VO_2 structure. The aforementioned resonance peak is a consequence of the stimulation of the surface plasmons initiated by the periodically arranged ring arrays in the four-cross structure.

The resonance frequency that is obtained from experimental measurements of gold/VO_2 design is similar to the simulations performed, where it is observed that the VO_2 thin film base adversely affects the resonant effect in the metamaterial structure.

The associated THz transmission alongside altering the conductivity of VO_2 through temperature, MIT nature was used to modulate their resonance frequencies. The agreement of the conclusion achieved from simulation estimates for these four-cross gold/VO_2 metamaterials based on both semiconducting and metallic VO_2 with those of the experimental measurements is outstanding.

THz transmission measurement and simulation results of gold four-cross patterned VO_2 film at 293 K (room temperature), which is much lower than MIT, is shown in Fig. 7 on the same graph. The initial simulation results that performed before experimental studies give a resonance peak at around 0.65 THz (Sim. 1 four-cross Gold-VO_2). It has been already known that the spectral response of metamaterial filters is sensitive to individual variation of each design parameters which can shift the peak frequency and bandwidth.

So, the simulation studies were repeated in compliance with measured unitcell parameters (Sim. 2 four-cross Gold-VO_2). If we compare the room temperature transmission intensity of gold four-cross patterned VO_2 film and four-cross patterned VO_2 film, it is around only 4% for second design with bare film. The modulation range is enhanced by 1 order magnitude in the four-cross patterned VO_2 film metamaterial structure so that the THz transmission can be fully switched off.

Mod. Phys. Lett. B Downloaded from www.worldscientific.com
by BILKENT UNIVERSITY on 01/03/24. Re-use and distribution is strictly not permitted, except for Open Access articles.

Mod. Phys. Lett. B Downloaded from www.worldscientific.com
by BILKENT UNIVERSITY on 01/03/24. Re-use and distribution is strictly not permitted, except for Open Access articles.

The low transmission intensity of the bare VO_2 layer can be attributed to the film thickness. The sharp alteration of refractive index in the course of the MIT process is the origin of the converse modulating tendency of transmittance with respect to temperature reported on thicker VO_2 films. The converse modulating tendency of transmittance could be induced by the debate in between transmittance and absorption rate.

Hence, possessing latent applications in the fields of THz imaging, sensing and communications the device under consideration is a thermally governable intensity modulator in the THz regime. The thin film quality can adversely affect the device efficiency. The optical characteristics of VO_2 films could be adjusted by numerous components some of which are structure, strain and defects. Well-controlled experimental condition is required in order to achieve the intended optical properties of VO_2 film and this necessity restricts its utilizations in manipulating waves. For instance, oxygen vacancy or unsought V valence states might be stimulated by spatially discriminative defect engineering or other sequential methods to produce VO_2 films. Accordingly, both the dielectric function and the effect of thickness of VO_2 film on the optical characteristics have to be taken under consideration.

The comparative analysis of this study with the previously published papers on metamaterial devices is given in Table 1. In this study, we used a four-cross structure that has many advantages over the reported studies, including a simple geometry, being easily fabricable., whereas the remaining designs either include multiple-stacked layers or nonswitchable characteristics, as compared to our proposed four-cross structure.

The complete form (unitcells are all connected to eachother) of the architecture also enables applying voltage to the metamaterial structure for the MIT. Both single

Table 1. Comparison among metamaterial devices.

Parameter	Unitcell size		Material	Device layers	Design configuration	Fabrication method	Switching ability
Ref. 40	∼nm	Absorber	Ni	Single	Nanocylinders	Nano imprint Lithography	—
Ref. 41	∼nm	Absorber	Au, Si	Multiple	Nanocones	Numerically demonstrated	—
Ref. 42	∼μm	Broadband absorber, Polarization converter, Filter	VO_2	Multiple	Four-layered structure of PI/VO_2/Au/PI With Au-VO_2 gratings	Photolithography	By MIT
Ref. 43	∼μm	Filter	Au, dielectric, VO_2	Multiple	Metal–VO_2–dielectric–metal-VO_2 (MVDMV)	Photolithography	By MIT
Ref. 44	∼μm	Absorber (metallic) Filter (Insulating)	Au, dielectric, VO_2	Multiple	Au/Polymide/VO_2/SiO_2	Numerically demonstrated	By MIT
Current Study	∼μm	Filter	Au, VO_2	Single Multiple	Four-cross Shaped (unit cells attached to each other)	Photolithography	By MIT

(four-cross-planar VO_2 device) and multiple layers (Au four-cross patterned VO_2 device) are used and compared in the study to understand the effect of design parameters on device performance.

This Au four-cross patterned VO_2 device with a temperature-dependent resonance behavior has great potential for tunable and low loss THz devices for imaging, sensing, and detection applications. By modifying the geometrical parameters of the four-cross structure and temperature-dependent MIT properties, the resonance frequency of the metamaterial structure can be switched. It provides to fabricate compact metamaterial-based filters with a high selectivity. These types of particular filters can be used to delete undesirable transmitted signals in pre-defined frequency bands and have potential applications in the field of THz diagnostics.

4. Conclusion

In summary, a thermally controllable THz metamaterial based on vanadium dioxide (VO_2) thin film was proposed. High quality DC magnetron sputtered VO_2 thin films were deposited and the resistivity change at transition temperature is approximately by a factor of four which is suitable for electrical switching applications. In this study, two different VO_2-based terahertz devices were introduced comprising metamaterials moreover their responses can be regulated by external stimulations. A unique four-cross metamaterial patterned above VO_2 films and on gold layer deposited on bare VO_2 layers by conventional μv lithography and ion beam etching techniques. In metamaterial filters, resonance switching and frequency shifting are observed depending on temperature. Accomplishment of a spectral tunability of the resonance by introducing VO_2 four-cross filters over the MIT temperature was demonstrated by consequences of simulations and THz-TDS measurements. Remarkably, in advance, the MIT happens to be evident at all, it is possible to control entirely the transmitting THz electromagnetic wave. The amplitude modulation stimulated by a temperature fluctuation of not more than 10°C across the MIT of VO_2 warrants for prolonging this design may support to accomplish excessive quality adjustable instruments for the THz region.

Acknowledgments

This work has been supported in part by TUBITAK (Scientific and Technological Research Council of Turkey) under project number 118F069. We would like to thank the Research and Application Center for Quantum Technologies (RACQUT) of IZTECH to perform some parts of the experiments.

References

1. M. Tonouchi, *Nat. Photonics* **1** (2007) 97.
2. I. Kawayama, C. Zhang, H. Wang and M. Tonouchi, *Supercond. Sci. Technol.* **26** (2013) I9 093002.
3. B. Ferguson and X.-C. Zhang, *Nat. Mater.* **1** (2006) 26.

Mod. Phys. Lett. B Downloaded from www.worldscientific.com
by BILKENT UNIVERSITY on 01/03/24. Re-use and distribution is strictly not permitted, except for Open Access articles.

Mod. Phys. Lett. B Downloaded from www.worldscientific.com
by BILKENT UNIVERSITY on 01/03/24. Re-use and distribution is strictly not permitted, except for Open Access articles.

4. L. Ozyuzer, A. E. Koshelev, C. Kurter, N. Gopalsami, Q. Li, M. Tachiki, K. Kadowaki, T. Yamamoto, H. Minami, H. Yamaguchi, T. Tachiki, K. E. Gray, W.-K. Kwok and U. Welp, *Science* **318** (2007) 1291.
5. Y. Demirhan, H. Alaboz, M. A. Nebioğlu, B. Mulla, M. Akkaya, H. Altan, C. Sabah and L. Ozyuzer, *Supercond. Sci. Technol.* **30** (2017) 7.
6. T. Semerci, Y. Demirhan, N. Miyakawa, H. B. Wang and L. Ozyuzer, *Opt. Quant. Electron.* **48** (2016) 340.
7. B.-X. Wang, C. Xu, G. Duan, W. Xu and F. Pi, *Adv. Funct. Mater.* **33** (2023) 2213818.
8. B.-X. Wang, C. Xu, G. Duan, W. Xu, J. Jiang, X. Wei and P. Fuwei, *Mater. Des.* **225** (111586) (2023) 0264.
9. B.-X. Wang, C. Xu, H. Zhou and G. Duan, *APL Mater.* **10**(5) (2022) 050701.
10. B. X. Wang, Y. He, P. Lou and W. Xing, *Nanoscale Adv.* **2** (2020) 763.
11. B.-X. Wang, W. Xu, Y. Wu, Z. Yang, S. Laia and L. Lu, *Nanoscale Adv.* **4**(5) (2022) 1359.
12. R. Singh, Z. Tian, J. Han, C. Rockstuhl, J. Gu and W. Zhang, *Appl. Phys. Lett.* **96**(7) (2010) 071114.
13. M. C. Ricci, H. Xu, R. Prozorov, A. P. Zhuravel, A. V. Ustinov and S. M. Anlage, *IEEE Trans. Appl. Supercond.* **17** (2007) 918.
14. C. H. Zhang, J. B. Wu, B. B. Jin, Z. M. Ji, L. Kang, W. W. Xu, J. Chen, M. Tonouchi and P. H. Wu, *Opt. Express* **20** (2012) 42.
15. H.-T. Chen, H. Yang, R. Singh, J. F. O'Hara, A. K. Azad, S. A. Trugman, Q. X. Jia and A. J. Taylor, *Phys. Rev. Lett.* **105** (2010) 247402.
16. F. J. Morin, *Phys. Rev. Lett.* **3** (1959) 34.
17. H.-T. Kim, B.-G. Chae, D.-H. Youn, G. Kim, K.-Y. Kang, S. J. Lee, K. Kim and Y. S. Lim, *Appl. Phys. Lett.* **86** (2005) 242101.
18. A. Pashkin, C. Küber, H. Ehrke, R. Lopez, A. Halabica, R. F. Haglund, R. Huber and A. Leitenstorfer, *Phys. Rev. B* **83** (2011) 195120.
19. A. Cavalleri, Th. Dekorsy, H. H. W. Chong, J. C. Kieffer and R. W. Schoenlein, *Phys. Rev. B* **70** (2004) 161102.
20. Y. Zhang, S. Qiao, L. Sun, Q. W. Shi, W. Huang, L. Li and Z. Yang, *Opt. Express* **22** (2014) 11070.
21. Y. G. Jeong, H. Bernien, J. S. Kyoung, H. R. Park, H. S. Kim, J. W. Choi, B.-J. Kim, H.-T. Kim, K. J. Ahn and D. S. Kim, *Opt. Express* **19** (2011) 21211.
22. M. Liu, H. Y. Hwang, H. Tao, A. C. Strikwerda, K. Fan, G. R. Keiser, A. J. Sternbach, K. G. West, S. Kittiwatanakul, J. Lu, S. A. Wolf, F. G. Omenetto, X. Zhang, K. A. Nelson and R. D. Averitt, *Nature* **487** (2012) 345.
23. S. B. Choi, J. S. Kyoung, H. S. Kim, H. R. Park, D. J. Park, Bong-Jun Kim, Y. H. Ahn, F. Rotermund, Hyun-Tak Kim, K. J. Ahn and D. S. Kim, *Appl. Phys. Lett.* **98** (2011) 071105.
24. Q.-Y. Wen, H.-W. Zhang, Z. Chen, Y. Long, Y.-L. Jing, Y. Lin and P.-X. A. Zhang, *J. Phys. D Appl. Phys.* **45** (2012) 235106.
25. P. U. Jepsen, B. M. Fischer, A. Thoman, H. Helm, J. Y. Suh, R. Lopez and R. F. Haglund, Jr., *Phys. Rev. B* **74** (2006) 205103.
26. T.-T. Lv, Y. X. Li, H. F. Ma, Z. Zhu, Z. P. Li, C. Y. Guan, J. H. Shi, H. Zhang, T. J. Cui, *Sci. Rep.* **6** (2016) 23186.
27. M. A. Kats, D. Sharma, J. Lin, P. Genevet, R. Blanchard, Z. Yang, M. M. Qazilbash, D. N. Basov, S. Ramanathan and F. Capasso, *Appl. Phys. Lett.* **101** (2012) 221101.
28. T. Driscoll, S. Palit, M. M. Qazilbash, M. Brehm and F. Keilmann, *Appl. Phys. Lett.* **93**(2) (2008) 024101.

29. H. Kim, N. Charipar, E. Breckenfeld, A. Rosenberg and A. Piqué, *Thin Solid Films* **596** (2015) 45.
30. K. Appavoo and R. F. Haglund Jr, *Nano Lett.* **11**(3) (2011) 1025.
31. M. J. Dicken *et al.*, *Opt. Express* **17**(20) (2009) 18330.
32. J. Zhang, W. Zhang, L. Zhang and S. A. Gu, *Solvent Extr. Ion Exch.* **32**(3) (2014) 221.
33. Y. Guo, H. Xu, C. Zou, Z. Yang, B. Tong, J. Yu, Y. Zhang, L. Zhao and Y. Wang, *J. Alloys Compd.* **622** (2015) 913.
34. X. He, J. Xu, X. Xu, C. Gu, F. Chen, B. Wu, C. Wang, H. Xing, X. Chen and J. Chu, *Appl. Phys. Lett.* **106** (2015) 093106.
35. J. R. Skuza, D. W. Scott and A. K. Pradhan, *J. Appl. Phys.* **118** (2015) 195303.
36. G. Fu, A. Polity, N. Volbers and B. K. Meyer, *Thin Solid Films* **515** (2006) 2519.
37. H. Yuce, H. Alaboz, Y. Demirhan, M. Ozdemir, L. Ozyuzer and G. Aygun, *Phys. Scr.* **92**(11) (2016) 114007.
38. H. Alaboz, Y. Demirhan, H. Yuce, G. Aygun and L. Ozyuzer, *Opt. Quantum Electron.* **49**(7) (2016) 238.
39. E. Amoupour, A. Abdolahzadeh, H. Ziabari, F. Andarva and E. Ghodsi, *Superlattices Microstruct.* **65**(332–343) (2014) 0749.
40. Y. Zhou, M. Luo, S. Shen, H. Zhang, D. Pu and L. Chen, *Opt. Express* **26** (2018) 27482.
41. N. T. Q. Hoa, P. H. Lam, P. D. Tung, T. S. Tuan and H. Nguyen, *IEEE Photonics J.* **11** (2019) 1.
42. Z. Chen, J. Chen, H. Tang, T. Shen and H. Zhang, *Opt. Mater. Express* **13** (2023) 514.
43. J. Huang, J. Li, Y. Yang, J. Li, Y. Zhang and J. Yao, *Opt. Commun.* **465**(125616) (2020) 0030.
44. Y. Wu, W. Xu, H. Zhou, X. Qiu, Y. He, Y. Gao and B.-X. Wang, *Appl. Phys. A* **128** (2022) 930.

Mod. Phys. Lett. B Downloaded from www.worldscientific.com
by BILKENT UNIVERSITY on 01/03/24. Re-use and distribution is strictly not permitted, except for Open Access articles.